RAPID COMMUNICATIONS

PHYSICAL REVIEW B VOLUME 44, NUMBER 18 1 NOVEMBER 1991-II

# Anharmonic local-moment fluctuations in the Hubbard model

W. Brenig, A. P. Kampf, H. Monien,* and J. R. Schrieffer
*Department of Physics, University of California, Santa Barbara, California 93106*
(Received 17 June 1991)

We investigate the role of anharmonic local-moment fluctuations in the two-dimensional Hubbard model for intermediate correlation strength in the regime of local-moment formation. Within a functional-integral scheme we perform a linked-cluster expansion of the effective action up to quartic order in the local-moment amplitudes. The resulting quadratic and quartic expansion coefficients are compared in real space and as a function of frequency, temperature, and chemical potential. We find the quartic contribution to suppress quadratic fluctuations and to be more susceptible to nesting than the quadratic term.

A key to the understanding of the high-temperature superconductors[1] is the effect of electron-electron correlation in the $CuO_2$ planes of the layered perovskite cuprates. This has become widely accepted after the two-dimensional, nearly half-filled Hubbard model[2] was proposed as the effective Hamiltonian[3] and experiments showed a correlation strength $U/4t$ of order unity.[4] Here $U$ denotes the on-site Coulomb repulsion and $t$ is the hopping energy. Despite the apparent simplicity of the Hubbard model and although techniques exist to treat the strongly and the weakly interacting limit,[5-7] no computational scheme for the relevant regime of intermediate correlations is known, and the interpolation between the two extreme limits remains an open question. Further complication arises through the rich low-temperature phase diagram of the model as a function of the hole doping relative to the half-filled case, including the antiferromagnetic insulator at very small doping, a spin-glass-like phase, and a strongly correlated electron liquid at intermediate doping concentrations.

The above emphasizes the need for novel theoretical approaches to the Hubbard model applicable to the range of intermediate coupling strength and doping. In this regime charge fluctuations are strongly suppressed due to the on-site Coulomb interaction. In contrast to this, local-moment fluctuations are significantly enhanced and, in addition, as one is near the antiferromagnetic instability, they develop medium-range correlations. It is important that these local-moment fluctuations are of large amplitude and experience strongly anharmonic dynamical restoring forces. An illustration for this is provided by the symmetric single-site Anderson model for $U\sim\Gamma$, where $\Gamma$ is the bare level width.[8,9] Here the free energy as a function of the local moment exhibits only a single minimum for $U\ll\Gamma$, but turns into a double well for $U\gg\Gamma$ as the local moment forms. Thus the essential signature of the intermediate coupling regime are anharmonic fluctuations of the effective exchange field. This in turn influences the single-particle properties as well as the spin-fluctuation spectrum. The main goal of the present work is to explore a functional-integral scheme capable of incorporating the effects of anharmonic local-moment fluctuations within correlated electronic systems. The paper is organized as follows. First, we outline the auxiliary field approach to the Hubbard model. Within this scheme we then introduce the relevant nonparabolic action functional by going beyond Gaussian order. To discuss this functional we perform a numerical evaluation of the relevant coupling terms involved and compare the Gaussian versus the non-Gaussian contributions. Finally, we state our conclusion.

In the following we concentrate on the partition function for the Hubbard model

$$H=-t\sum_{\langle i,j\rangle,\sigma}c_{i\sigma}^{\dagger}c_{j\sigma}+U\sum_{i}n_{i\uparrow}n_{i\downarrow}\,, \tag{1}$$

where $\langle i,j\rangle$ refers to nearest-neighbor sites, $c_{i\sigma}^{\dagger}$ and $c_{j\sigma}$ create and destroy fermions on the two-dimensional square lattice, respectively, and $n_{i\sigma}=c_{i\sigma}^{\dagger}c_{i\sigma}$ is the local density for spin $\sigma$. We want to focus on the spin density as the dominant collective coordinate of the system. This is achieved by the Hubbard-Stratonovich transformation,[10] which maps the partition function of an interacting many-body system onto that of a single-particle problem in the presence of an auxiliary $c$-number field with Gaussian fluctuations. This mapping is not unique,[9,11] reflecting the freedom of choice of a particular collective coordinate. Using the continuous Ising field representation, one obtains the following functional integral:[9,11]

$$Z=\int D[x]\,\mathrm{Tr}\left\{T_{\tau}\exp\left[-\int_{0}^{\beta}\left(\frac{U}{2}\sum_{i}x_i^2(\tau)+H(\{x\})\right)d\tau\right]\right\}, \tag{2}$$

$$H(\{x\})=-t\sum_{\langle i,j\rangle,\sigma}c_{i\sigma}^{\dagger}c_{j\sigma}-U\sum_{i,\sigma}\sigma x_i(\tau)n_{i\sigma}-\mu N\,.$$

Here $\beta=1/T$ is the inverse temperature, $N$ is the total particle number operator, and $\mu=\mu_0-U/2$ is a renormalized chemical potential. The auxiliary fields are denoted by $x_i(\tau)$, where $i$ labels the lattice site and $\tau$ is the imaginary time. Equation (2) represents a one-particle problem, with $x_i(\tau)$ playing the role of the fluctuating, site-diagonal exchange field. Although Eq. (2) refers to a particular spin-quantization direction, the functional integration restores the spin rotational invariance. Taking the

 

trace over the fermion degrees of freedom leads to[12]

$$Z = Z_0 \int D[x] \exp[A(\{x\})] ,$$

$$A(\{x\}) = -\frac{\beta U}{2} \sum_{i,\omega_l} |x_i(\omega_l)|^2 + \mathrm{Tr} \ln(\underline{1} - \underline{M}) . \quad (3)$$

Here $A(\{x\})$ represents the action functional. $Z_0$ is the partition function of the noninteracting system, $x_i(\omega_l)$ is the Fourier transform of $x_i(\tau)$ where $\omega_l = 2\pi l T$, and $l$ is an integer. The remaining trace in $A(\{x\})$ refers to a matrix in real, frequency, and spin space where $\underline{M}$ is defined by

$$\underline{M}^{\sigma\sigma'}_{\omega_l+\nu_n,\nu_n|i,j} = -\sigma \delta_{\sigma\sigma'} U x_i(\omega_l) G_{ij}(\nu_n) . \quad (4)$$

In Eq. (4) we have introduced the lattice Green's functions $G_{ij}(\nu_n)$ for the two-dimensional tight-binding model,[13] where $i,j$ label sites of the two-dimensional square lattice and $\nu_n = (2n+1)\pi T$.

A standard way to evaluate Eq. (3) is to treat only the Gaussian fluctuations of the $x$ fields around a saddle point of $A(\{x\})$, i.e., the random-phase approximation (RPA). Since this approach is restricted to an action functional which is dominated by harmonic fluctuations about a single absolute minimum in the exchange field configuration space, it is insufficient for intermediate values of $U/t$ where, due to local-moment formation *large amplitude, anharmonic,* and *slow* mode fluctuations of the $x$ fields play the important role. For a proper description of this regime one has to retain the non-Gaussian terms in $A(\{x\})$. To pursue this point, which is motivated by the single-site Anderson problem, we have investigated the quartic contributions to $A(\{x\})$. The action up to fourth order in $x_i(\omega_l)$ is given by

$$A_4(\{x\}) = -\frac{U}{2T} \sum |x_i(\omega_l)|^2 - \frac{U^2}{T} \sum K_2(i,\omega_l|p) x_i(\omega_l) x_p(-\omega_l)$$
$$- \frac{U^4}{2T} \sum K_4(i,\omega_l|j,\omega_m|k,\omega_n|p) x_i(\omega_l) x_j(\omega_m) x_k(\omega_n) x_p(-\omega_S) , \quad (5)$$

where $\omega_S = \omega_l + \omega_m + \omega_n$ and the summation is implied to run over the respective lattice sites and Matsubara frequencies. $K_2$ and $K_4$ are obtained by the standard linked-cluster expansion of $A(\{x\})$:[12]

$$K_2(i,\omega_l) = T \sum_{\nu_n} G_{i0}(\nu_n + \omega_l) G_{0i}(\nu_n) ,$$

$$K_4(i,\omega_l|j,\omega_m|k,\omega_n) = 2T \, \mathrm{Re} \sum_{\nu_n} [G_{i0}(\nu_n) G_{ji}(\nu_n + \omega_l) G_{kj}(\nu_n + \omega_l + \omega_m) G_{0k}(\nu_n + \omega_S)$$
$$+ G_{i0}(\nu_n) G_{ki}(\nu_n + \omega_l) G_{jk}(\nu_n + \omega_l + \omega_n) G_{0j}(\nu_n + \omega_S)$$
$$+ G_{j0}(\nu_n) G_{ij}(\nu_n + \omega_m) G_{ki}(\nu_n + \omega_l + \omega_m) G_{0k}(\nu_n + \omega_S)] . \quad (6)$$

Translational symmetry has been used to fix the site $p$ in Eq. (5) at the origin denoted by the subscript "0." Note that $A_4(\{x\})$, as well as $K_2$ and $K_4$, are real quantities and that $K_4$ is symmetric under permutations of any of the vertex pairs $i,\omega_l \leftrightarrow j,\omega_m$.

In the following our main objective is to understand the properties of $K_4$ and the interplay between the quadratic and the quartic term in $A_4(\{x\})$. Thus we have performed the frequency sums in Eq. (6) numerically. Since local effects are most interesting for the relevant parameter range of the doping concentration and $U/4t$, the lattice Green's functions $G_{lm}(\nu_n)$ form the appropriate representation. Values for these lattice Green's functions can be obtained by exploiting their relation to the first and second elliptic integrals through a set of recursion equations.[13]

Before treating the lattice it is instructive to apply Eqs. (5) and (6) to the simpler case of a two-site Hubbard model. Choosing a *particular* path $\{x\}_P$ in the configuration space one may compare the exact action $A(\{x\}_P)$ obtained from Eqs. (2) with an expansion similar to Eq. (5). In this case $K_2$ and $K_4$ can be evaluated analytically. Figure 1 shows the result for the path: $x_1(\tau) = -x_2(\tau) = (\delta\xi_0/2)\sin(\omega_n \tau)$ for the parameters $\beta t = 10$ and $U/t = 4$. In the figure we have subtracted the "bare" Gaussian contribution from the expansion, as well as from the exact result. It is evident that for small amplitude fluctuations the RPA is a reasonable approximation for all frequencies. For large amplitudes and low frequencies the RPA overestimates the fluctuation contribution to the exact action $A(\{x\}_P)$. The inset demonstrates that this tendency of the RPA is counteracted by the quartic contribution, which has a *sign opposite to the quadratic term* and is restricted to lower frequencies. This results in good

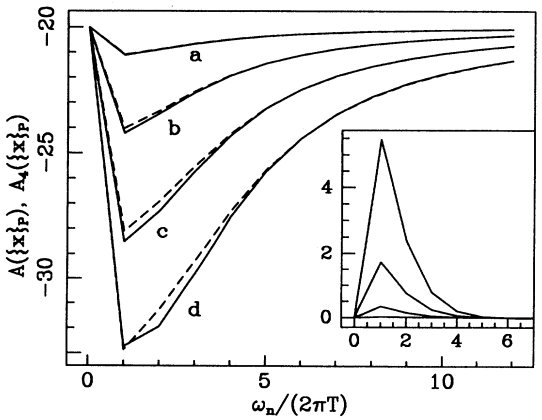


FIG. 1. The quartic approximation to the action $A_4(\{x\}_P)$ (solid lines) compared with the exact result $A(\{x\}_P)$ (dashed lines) for the two-site model and the particular path $P$: $x_1(\tau) = -x_2(\tau) = (\delta\xi_0/2)\sin(\omega_n \tau)$. Inset: The $K_4$ contribution to $A_4(\{x\}_P)$. $\beta t = 10$, $U/t = 4$, and the labels $a$, $b$, $c$, and $d$ refer to $\delta\xi_0 = 0.25$, 0.5, 0.75, and 1.0, respectively.

agreement between $A(\{x\}_P)$ and $A_4(\{x\}_P)$ for the range of parameters we have used in Fig. 1.

Turning to the lattice, we first compare the real-space structure of $K_2$ and $K_4$ in the *static limit*. As $K_4$ depends on two more coordinates than $K_2$ we select those $K_4$ with only two independently chosen sites. There are two dominant configurations of this type since $G_{ij}(\nu_n)$ decreases rapidly as a function of the distance between $i$ and $j$. One is obtained by equating three sites, $j=k=p$, leaving the fourth, $i$, independent. The other is given by contracting the vertices pairwise, $i=j$ and $k=p$, onto two independent sites. We find both contributions to behave similarly in real space.

In Fig. 2 we keep $j$, $k$, and $p$ at the origin and vary $i$ along the $x$ direction or the diagonal, respectively. For simplicity we have assumed the doping concentration $\delta$ to be zero: $\mu=0$. The temperature is set to $T=0.01$, where the hopping matrix element has been normalized to unity $t=1$. Obviously, $K_4$ is of *opposite sign,* and *counteracts* $K_2$ for all sites—including those which are not depicted. The real-space structure of the signs is in accordance with long-range, commensurate antiferromagnetic (AFM) correlations at $\delta=0$. For $\delta\neq 0$ we find that the competition between $K_2$ and $K_4$ remains valid, but AFM correlations are commensurate only within a shorter range. Note that $K_2$ and $K_4$ extend further along the diagonal, where $K_4$ is of longer range, than along the $x$ direction for the given value of the chemical potential. This is the real-space signature of nesting. Since $K_4$ contains a product of four Green's functions it is even *more susceptible* to nesting than $K_2$. For doping concentrations $\delta\gtrsim 0.2$ one finds $K_2$ and $K_4$ to be short ranged in all directions.

In Fig. 3 we compare the temperature and the chemical-potential dependence of the *static on-site* values of $K_2$ and $K_4$. One observes that $K_4$ is very sensitive to variations of the temperature at zero doping and the chemical potential at a moderately low temperature. In contrast to that $K_2$ depends only weakly on these parameters. Figure 4 demonstrates the frequency dependence of the *on-site* values of $K_2$ and $K_4$. Analogous to the real-space situation only one of the independent frequencies of $K_4$ is varied. The remaining two are chosen to be zero. The temperature has been set to $T=0.01$ and the chemical potential to $\mu=-0.1$. Both the quadratic and the quartic term fall off on a scale of the order of the bandwidth, as expected. In addition, $K_4$ decays more rapidly than $K_2$. This is clear also from the high-frequency expansions of the expressions in Eq. (6). These features are reminiscent of the two-site case.

Finally, we comment on the magnitude of the quadratic versus the quartic contribution. First, it is clear from Eq. (3) that the mean-square value $\langle|x_i(\omega_l)|^2\rangle$ of a typical $x_i(\omega_l)$ will be of order $T/U$ in the paramagnetic phase. Second, Fig. 4 suggests that each frequency sum over $K_2$ and $K_4$ in Eq. (5) contributes approximately $t/T$ similar terms. Third, the functional integration contracts the $x$ fields, reducing the number of frequency sums in the quartic contribution effectively by 1. Thus an estimate of the

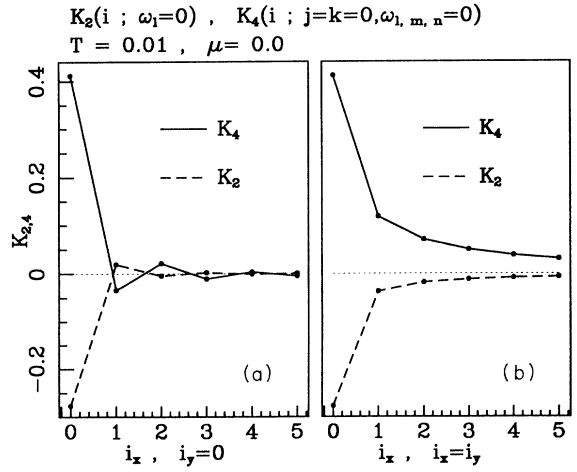


FIG. 2. Real-space dependence of $K_2$ and $K_4$ for $j=k$ at the origin and $i$ varying along (a) the $x$ direction and (b) the diagonal, respectively. The lattice constant $a$ and the hopping matrix element $t$ are normalized to 1.

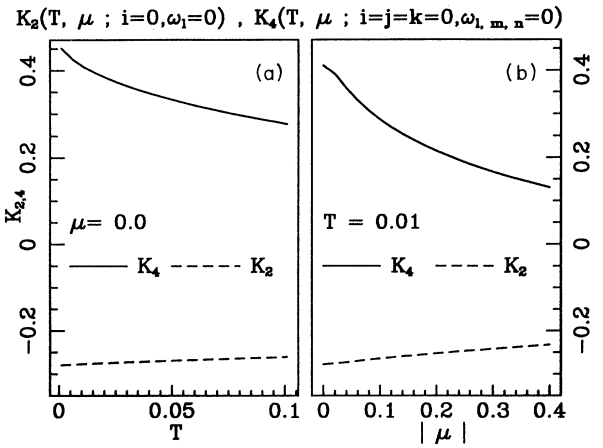


FIG. 3. (a) Typical temperature and (b) chemical-potential dependence of the static on-site terms $K_2$ and $K_4$. ($t=1$.)

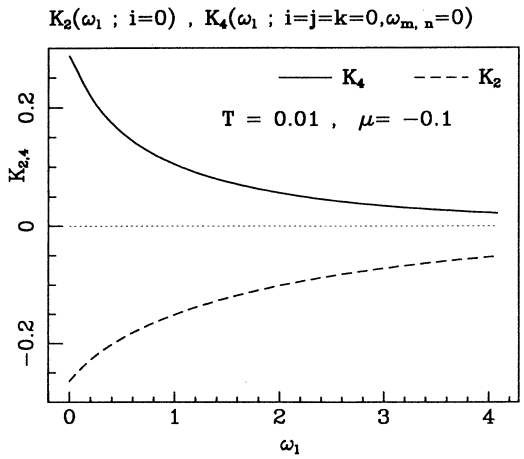


FIG. 4. Frequency dependence of the on-site terms $K_2$ and $K_4$ for $\omega_m=\omega_n=0$. ($t=1$.)

relative weight of $K_4$ vs $K_2$ within the path integration can be inferred from Figs. 2, 3, and 4 by multiplying the value of $K_4$ given in the figures with a factor of order $U/t \sim O(1)$.

In conclusion, we have emphasized the anharmonic nature of the action functional for the Hubbard model in the configuration space of local-moment amplitudes within the regime of intermediate correlation strength. In particular, we find that the quartic term in the action opposes the RPA instability and is even more sensitive to nesting than the quadratic term. Thus we expect that large amplitude, non-Gaussian local-moment fluctuations will strongly influence the single-particle spectrum as well as the low-frequency dynamical spin susceptibility. The full single-particle Green's function $\mathcal{G}_{ij}(\nu_n)$ is given by the average of the Green's function for given $x$ fields $\langle \mathcal{G}_{ij}^{[x]}(\nu_n) \rangle$ using the distribution implied by Eq. (2) and the spin susceptibility $\chi_{ij}(\omega_n)$ is proportional to $[\beta U \langle x_i(\omega_l) x_j(-\omega_l) \rangle - \delta_{ij}]$.[11] Equations (3) and (5) provide a convenient starting point for the evaluation of such average values within the framework of classical Monte Carlo techniques. Future investigations should include the effect of renormalizations on the quadratic and the quartic terms. In addition, it will be interesting to compare the above calculation using the itinerant picture with an expansion analogous to Eq. (5) but starting from the atomic limit.

Partial support for this work was provided by NSF Grant No. DMR 89-18307, by EPRI Grant No. EPRIRP-8009-18, and by NSF Grant No. PHY 89-04035. One of us (H.M.) is grateful for partial support by IBM. W.B. gratefully acknowledges support by the Max-Planck-Gesellschaft.

---

*Also at Institute for Theoretical Physics, University of California, Santa Barbara, CA 93106.

[1] J. G. Bednorz and K. A. Müller, Z. Phys. B **64**, 189 (1986).

[2] M. C. Gutzwiller, Phys. Rev. Lett. **10**, 159 (1963); J. Hubbard, Proc. R. Soc. London, Ser. A **276**, 238 (1963).

[3] P. W. Anderson, in *Frontiers and Borderlines in Many Particle Physics,* Proceedings of the International School of Physics "Enrico Fermi," Course CIV, Varenna, 1987, edited by R. A. Broglia and J. R. Schrieffer (North-Holland, Amsterdam, 1988).

[4] J. Fink, J. Pflüger, Th. Müller-Heinzerling, N. Nücker, B. Scheerer, H. Romberg, M. Alexander, R. Manzke, T. Buslaps, R. Claessen, and M. Skiboswski, in *Earlier and Recent Aspects of Superconductivity,* edited by J. G. Müller and K. A. Bednorz (Springer-Verlag, Berlin, 1990).

[5] E. Dagotto, Int. J. Mod. Phys. B **5**, 77 (1991), and references therein.

[6] N. Bulut, D. Hone, D. J. Scalapino, and N. E. Bickers, Phys. Rev. Lett. **64**, 2723 (1990); N. Bulut, in *Proceedings of the NATO ARW on the Dynamics of Magnetic Fluctuations in HTCS,* Crete, edited by G. Reiter, P. Horsch, and Psaltakis (Plenum, New York, 1990).

[7] A. J. Millis, H. Monien, and D. Pines, Phys. Rev. B **42**, 167 (1990).

[8] J. R. Schrieffer, W. E. Evenson, and S. Q. Wang, J. Phys. (Paris) Colloq. **1**, C-19 (1971).

[9] W. E. Evenson, J. R. Schrieffer, and S. Q. Wang, J. Appl. Phys. **41**, 1199 (1970).

[10] R. L. Stratonovich, Dokl. Akad. Nauk SSSR **115**, 1097 (1957) [Sov. Phys. Dokl. **2**, 416 (1958)]; J. Hubbard, Phys. Rev. Lett. **3**, 77 (1959).

[11] J. R. Schrieffer (unpublished).

[12] J. W. Negele and H. Orland, *Quantum Many-Particle Systems, Frontiers in Physics* (Addison-Wesley, Reading, MA, 1988).

[13] T. Morita, J. Math. Phys. **12**, 1744 (1971).